Available online www.jsaer.com

***Journal of Scientific and Engineering Research*, 2017, 4(4):74-85**

Research Article

ISSN: 2394-2630
CODEN(USA): JSERBR

Inverted Pendulum Control using Adaptive Manifold Immersion (Part-I: Continuous Time Design)

Qasim Javaid, Syed A. Ahmed, Mubashir Ali, Ammar Tanveer

Department of Electrical Engineering, COMSATS Institute of Information Technology, Wah-47040, Pakistan

Abstract This article describes a novel controller design for the inverted pendulum system using nonlinear robust adaptive immersion method. The system dynamics are modelled and converted to geometric control notation. The full order system is compensated by a controller designed for a reduced order exosystem. The controller designed is based on the immersion of C_∞ manifolds. The continuous time control algorithm is simulated in Matlab/Simulink. The viability of the proposed controller is theoretically and experimentally demonstrated by the promising behavior of the system starting from any initial condition and hence guaranteeing the wider operating region of the system.

Keywords Inverted Pendulum, Immersion, Invariance, Robust Adaptive Control, Rapid Control Prototyping

Introduction

The inverted pendulum platform is among challenging control systems. This platform has been a benchmark to practice various control techniques. A lot of research work has been dedicated to this system owing to highly nonlinear and complex dynamic structure of this system. The literature addresses techniques such as standard linearization approaches, decoupled neural network reference compensation techniques, Lyapunov function methods, computer vision-based control, adaptive fuzzy controls, based controls etc. [1-2]. Since most of the real-world systems are non-linear with parameter uncertainties, so most of the aforementioned techniques result in performance degradation with the parameter uncertainties and also impose the narrow operating range constraints [3-4]. One solution to this problem is sliding mode control [5]. Sliding mode control involves the development of discontinuous control laws that make the dynamics of a system evolve on an attractive sliding manifold [6]. Moreover, sliding mode algorithm requires sliding surface to be reached [4]. We have modified and extended the continuous control algorithm, which does not necessarily require target submanifold to be reached and it is robust against parameter uncertainties as compared to optimal control approach [7] that intrinsically suffers the drawback of deterioration in system performance with plant parameter uncertainties.

The adaptive immersion based control approach is intuitive and it has growing trends [3, 6]. We have adopted this approach to define an exosystem evolving on a submanifold in the state space of the plant. This subspace contains the zero equilibrium of the plant. A control algorithm is synthesized that makes this submanifold attractive for initial conditions "off" this submanifold by using formulations.

System Dynamics and Problem Formulation

The plant consists of an inverted pendulum in the form of a rod. A cylindrical mass is attached to one end of this rod and the other end is hinged to a cart capable of moving back and forth on a railing by means of a pulley-belt mechanism. The pulley is rotated by a PMDC motor. The experimental setup is shown in Figure 1.

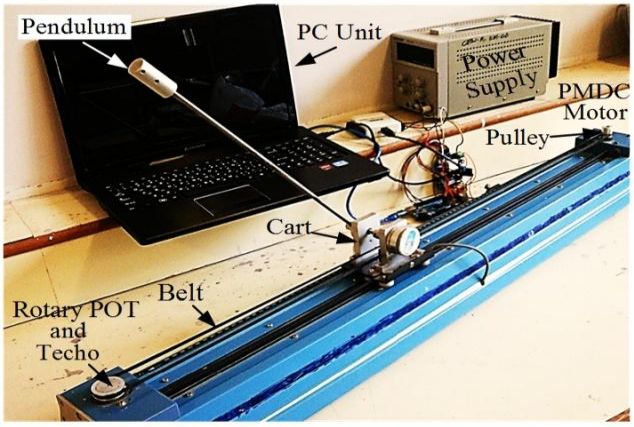

Figure 1: The experimental setup

The position and velocity of the cart are measured by rotary potentiometer and tachometer respectively, coupled to the belt as shown in Figure 1. The acceleration of the cart is measured by accelerometer on an inertial measurement unit (IMU) board attached to the cart. Pendulum angle θ and angular velocity $d\theta / dt$ are measured by rotary potentiometer and MEMS rate gyro respectively, attached to the axel at the hinge of the pendulum base as shown in Figure 2.

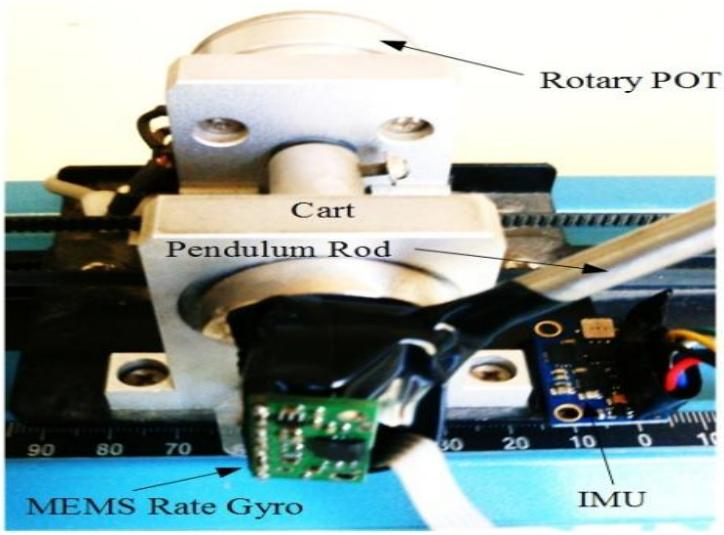

Figure 2: The sensing mechanism

If x and θ denote the position of the cart and angular displacement of the pendulum respectively, then pendulum cart assembly dynamics can be described by nonlinear differential system given by Equation 1 and Equation 2.

$$\left(m + Msin^2\theta\right)\ddot{x} - ml\dot{\theta}^2 sin\theta + \frac{mg}{2} sin\left(2\theta\right) = F_c \tag{1}$$

$$M\ddot{x}cos\theta - ml\ddot{\theta} = mgsin\theta \tag{2}$$

Here F_c is the force on the cart. The description of the various other system parameters in above modeling equations are given in Table 1 [8]. The dynamics of the PMDC motor are given by system of Equation 3 [9, 10].

$$\begin{aligned} e_a &= R_a i_a + k_m \dot{\phi} \\ J\ddot{\phi} &= \tau_a - B_R\dot{\phi} - \tau_p \end{aligned} \tag{2}$$

Here τ_a is the torque produced in the armature, τ_p is load torque on pulley resulting from fetching of cart, J is the moment of inertia of armature and pulley assembly, ϕ is the angular displacement of armature shaft and e_a is the voltage applied to the motor.

Table 1 Description and numerical values of the system parameters.

Parameter Description	Symbol	Value
Acceleration due to Gravity (m/sec2)	g	9.8
Moment of Inertia (Kg.m2)	J	1.69e-5
Point mass of the pendulum (Kg)	m	0.060
Mass of the PMDC motor rotor (Kg)	m_R	0.050
Mass of the cart (Kg)	M	0.400
Mass of the pulley (Kg)	m_p	0.025
Diameter of pulley (m)	D	0.060
Radius of PMDC motor rotor (m)	r_R	0.015
Radius of the pulley (m)	r_p	0.030
Length of pendulum (m)	l	0.350
Rotary friction constant for rotor-pulley assembly (Nm/rad/sec)	B_R	0.08
Rotor resistance (Ω)	R_a	0.8
Torque constant of the motor (N.m/A)	κ_τ	0.008
Velocity (back-emf) constant of the motor (V/rad/sec)	κ_m	0.015
System parameter	k_1	28.0
System parameter	k_2	19.048

Various coupling relations are given by Equation 4.

$$\begin{aligned} \tau_a &= k_\tau i_a \\ \tau_p &= DF_c \\ x &= r_p \phi \end{aligned} \tag{4}$$

Using Equation 1 and Equation 4, we get Equation 5.

$$\ddot{x} = \frac{1}{a_1 + a_2 \sin^2\theta}\left[a_3\dot{\theta}^2 sin\theta - a_4 sin(2\theta) - a_5\dot{x} + a_6 e_a\right] \tag{5}$$

The values of the various constants in Equation 5 are given in Table 2.

Table 2: Expressions and values of a_i constants.

Parameter Description	Symbol	Value
a_1	Dm	0.0036
a_2	DM	0.0240
a_3	Dml	0.0013
a_4	$Dmg/2$	0.0176
a_5	$(1/r_p)(k_m + k_\tau/R_a)$	2.6717
a_6	k_τ/R_a	0.0100

We apply partial feedback linearization control law of Equation 6,

$$e_a = \frac{1}{a_6}\left[\left(a_1 + a_2 \sin^2\theta\right)u - a_3\dot{\theta}^2 sin\theta + a_4 sin\left(2\theta\right) + a_5\dot{x}\right] \tag{6}$$

Using Equation 2, Equation 5 and Equation 6 and defining $k_1 = g/l$ and $k_2 = M/(lm)$, we get the system dynamics given by set of Equations 7.

$$\begin{aligned} \ddot{\theta} &= k_1 sin\theta - k_2 \ddot{x} cos\theta \\ \ddot{x} &= u \end{aligned} \tag{7}$$

Adaptive Manifold Immersion

Geometric Nonlinear System Model

Let's define state vector for system in Equation 7 as,

$$\underline{p} = \begin{bmatrix} p_1 & p_2 & p_3 \end{bmatrix}^{\mathrm{T}} = \begin{bmatrix} \dot{x} & \theta & \dot{\theta} \end{bmatrix}^{\mathrm{T}} \tag{8}$$

Using Equation 7 and Equation 8, we can describe our system in form of Equation 9 that is suitable for geometric nonlinear control approach.

$$\dot{\underline{p}} = \underline{f}\left(\underline{p}\right) + \underline{g}\left(\underline{p}\right)u = \underline{s}\left(\underline{p}, u\right) \tag{9}$$

The state vector $\underline{p}$ evolves on a smooth manifold P of dimension 3, which is spanned by tangential manifold to system map $\underline{s}$. In Equation 10 the system map $\underline{s}$ is decomposed into drift vector field $\underline{f}(\cdot)$ and controlled vector field $\underline{g}$. Using Equation 7 and Equation 8, these system mappings are given by Equation 10.

$$\begin{aligned} \underline{f}\left(\underline{p}\right) &= \begin{bmatrix} 0 & p_3 & k_1 sinp_2 \end{bmatrix}^T \\ \underline{g}\left(\underline{p}\right) &= \begin{bmatrix} 1 & 0 & -k_2 cosp_2 \end{bmatrix}^T \\ \underline{s}\left(\underline{p}, u\right) &= \begin{bmatrix} u & p_3 & k_1 sin\theta - k_2 ucos\theta \end{bmatrix}^T \end{aligned} \tag{10}$$

Here $u \in U\left(\underline{p}\right)$ is the system forcing function. U is a state dependent input set which belongs to the control bundle $u \in \bigcup_{\underline{p} \in P} U\left(\underline{p}\right)$.

Continuous Time Controller Design

We define an exosystem in terms of state vector $\underline{q} \in \mathrm{R}^2$, which contains origin in its reachable set. This can be achieved by defining the vector field of exosystem $\underline{\Upsilon}\left(\underline{q}\right)$ that governs the evolution of $\underline{q}$ as given by Equation 11.

$$\dot{\underline{q}} = \underline{\Upsilon}\left(\underline{q}\right) \tag{11}$$

We define a smooth submanifold for exosystem in Equation 11 as,

$$Q = \left\{\underline{p} \in \mathrm{R}^n \mid \underline{p} = \underline{\psi}\left(\underline{q}\right); \underline{q} \in \mathrm{R}^q\right\} \tag{12}$$

The controlled integral curves of system map $\underline{s}$ can be attracted by the submanifold Q if partial differential Equation 13 along with condition in Equation 14 is satisfied.

$$\underline{f}\left(\underline{\psi}\left(\underline{q}\right)\right)+\underline{g}\left(\underline{\psi}\left(\underline{q}\right)\right)\wp\left(\underline{\psi}\right)=L_{\underline{\Upsilon}}\underline{\psi} \tag{13}$$

$$\underline{q}\left(t\right)=\underline{0}\,\forall\,\underline{q}\left(0\right)\in \mathrm{R}^{q}\; as\, t\to\infty \tag{14}$$

Here $L_{\underline{\Upsilon}}\underline{\psi}=\left(\nabla_{\underline{q}}\underline{\psi}\right)\underline{\Upsilon}\left(\underline{q}\right)$ is the so-called Lie derivative. Also $\wp\left(\underline{\psi}\left(\underline{q}\right)\right)=\vartheta\left(\underline{\psi}\left(\underline{q}\right),0\right)$ on the submanifold Q and $u=\vartheta\left(\underline{p},\zeta\left(\underline{p}\right)\right)$ is the synthesized feedback control law that renders Q attractive. $\zeta(\cdot)$ is the implicit description of Q, which is given by parameterized form in Equation 12.

$$\zeta\left(\underline{p}\right)=\underline{p}-\underline{\psi}\left(\underline{q}\right)=0 \tag{15}$$

We introduce state variable $\hbar$ to define "off" the submanifold Q dynamics given by,

$$\dot{\underline{\hbar}}=L_{\underline{s}}\,\zeta\big|_{u=\vartheta\left(\underline{p},\hbar\right)}=\frac{\partial\zeta}{\partial\underline{p}}\,\underline{s}\left(\underline{p},\vartheta\left(\underline{p},\hbar\right)\right) \tag{16}$$

In terms of $\hbar$ and the synthesized controller ϑ, system mapping is given by,

$$\dot{\underline{p}}=\underline{s}\left(\underline{p},\vartheta\left(\underline{p},\hbar\right)\right) \tag{17}$$

Now we develop Equation 11 through Equation 17 for our control problem and analyse the stability. We select an exosystem Equation 11 given by Equation 18.

$$\begin{aligned}\dot{q}_1&=q_2\\ \dot{q}_2&=\beta\left(q_1,q_2\right)\end{aligned} \tag{18}$$

Defining the mapping $\underline{\psi}(\cdot)$ in Equation 12 as,

$$\underline{\psi}\left(\underline{q}\right)=\begin{bmatrix}\psi_1\left(q_1,q_2\right)\\ q_1\\ q_2\end{bmatrix} \tag{19}$$

Evaluating Equation 13 and $L_{\underline{\Upsilon}}\underline{\psi}$ using Equation 18 and Equation 19, we get Equation 20.

$$\begin{bmatrix}0\\ q_2\\ k_1 sin\left(q_1\right)\end{bmatrix}+\begin{bmatrix}1\\ 0\\ -k_2 cos\left(q_1\right)\end{bmatrix}\wp\left(\underline{\psi}\right)=\begin{bmatrix}\partial\psi_1/\partial q_1 & \partial\psi_1/\partial q_2\\ 1 & 0\\ 0 & 1\end{bmatrix}\begin{bmatrix}q_2\\ \beta\left(q_1,q_2\right)\end{bmatrix} \tag{20}$$

The matrix Equation 20 evaluates to Equation 21.

$$\begin{aligned} \wp\left(\underline{\psi}\right) &= \frac{\partial \psi_1}{\partial q_1} q_2 + \frac{\partial \psi_1}{\partial q_2} \beta\left(q_1, q_2\right) \\ k_1 sin\left(q_1\right) - k_2 cos\left(q_1\right) \wp\left(\underline{\psi}\right) &= \beta\left(q_1, q_2\right) \end{aligned} \tag{21}$$

We get the expression for the mapping β from Equation 21 that is given by Equation 22.

$$\beta\left(q_1, q_2\right) = \frac{k_1 sin\left(q_1\right) - k_2 q_2 cos\left(q_1\right) \frac{\partial \psi_1}{\partial q_1}}{1 + k_2 cos\left(q_1\right) \frac{\partial \psi_1}{\partial q_2}} \tag{22}$$

Let us define the following function in Equation 23.

$$\begin{aligned} \beta_1\left(q_1\right) &= -k_1 sin\left(q_1\right) \\ \beta_2\left(q_1, q_2\right) &= k_2 q_2 cos\left(q_1\right) \frac{\partial \psi_1}{\partial q_1} \\ \beta_3\left(q_1\right) &= 1 + k_2 cos\left(q_1\right) \frac{\partial \psi_1}{\partial q_2} \end{aligned} \tag{23}$$

We have made the assumption in Equation 24 in defining β_3, making it a function of q_1. It makes the calculations simpler without loss of generality.

$$\frac{\partial \psi_1}{\partial q_2} = \frac{\partial \psi_1}{\partial q_2}\left(q_1\right) \tag{24}$$

We get the decomposed form of Equation 22 using definitions in Equation 23 as,

$$\beta\left(q_1, q_2\right) = -\frac{\beta_1\left(q_1\right)}{\beta_3\left(q_1\right)} - \frac{\beta_2\left(q_1, q_2\right)}{\beta_3\left(q_1\right)} \tag{25}$$

Using Equation 19 and Equation 15, we get the expression for ζ given by Equation 26.

$$\zeta\left(\underline{p}\right) = \underline{p}_1 - \psi_1\left(p_2, p_3\right) = 0 \tag{26}$$

Noting that,

$$\nabla_{\underline{p}} \zeta = \begin{bmatrix} 1 \\ -\partial \psi_1 / \partial p_2 \\ -\partial \psi_1 / \partial p_3 \end{bmatrix} \tag{27}$$

Using Equation 26 and Equation 27, the Equation 16 evaluates to Equation 28.

$$\dot{\underline{\hbar}} = \vartheta\left(\underline{p}, \hbar\right)\left(1 + k_2 cos\left(p_2\right) \frac{\partial \psi_1}{\partial p_3}\right) - k_1 sin\left(p_2\right) \frac{\partial \psi_1}{\partial p_3} - p_3 \frac{\partial \psi_1}{\partial p_2} \tag{28}$$

Selecting $\dot{\hbar} = -\alpha\hbar$ renders submanifold Q attractive. With this choice and using Equation 28, we get control input given by Equation 29.

$$\vartheta\left(\underline{p},\hbar\right) = \frac{-\alpha\hbar + k_1 sin\left(p_2\right)\frac{\partial\psi_1}{\partial p_3} + p_3\frac{\partial\psi_1}{\partial p_2}}{1 + k_2 cos\left(p_2\right)\frac{\partial\psi_1}{\partial p_3}} \tag{29}$$

Using Equation 25 and Equation 29, exosystem can be described as,

$$\begin{aligned} \dot{\hbar} &= -\alpha\hbar \\ \dot{p}_2 &= p_3 \\ \dot{p}_3 &= \frac{1}{\beta_3\left(p_2\right)}\left[-\beta_1\left(p_2\right) - \beta_2\left(p_2, p_3\right) + \alpha cos\left(p_2\right)\hbar\right] \end{aligned} \tag{30}$$

To analyse the stability of exosystem in Equation 30, we define Lyapunov function *E* given by Equation 31, for some $\delta_1 > 0$ and $\delta_2 > 0$.

$$E = \frac{1}{2}p_3^2 + \int\frac{\beta_1\left(p_2\right)}{\beta_3\left(p_2\right)}dp_2 + \frac{\alpha}{2\delta_1^2\delta_2}\hbar^2 \tag{31}$$

To ensure that *E* is positive definite (locally) near origin, we observe that,

$$\left.\frac{\beta_1\left(p_2\right)}{\beta_3\left(p_2\right)}\right|_{p_2=0} = 0 \tag{32}$$

$$\frac{d}{dp_2}\left(\left.\frac{\beta_1\left(p_2\right)}{\beta_3\left(p_2\right)}\right|_{p_2=0}\right) = -\frac{k_1}{\left.\beta_3\left(p_2\right)\right|_{p_2=0}} \tag{33}$$

Let us assume,

$$\left.\beta_3\left(p_2\right)\right|_{p_2=0} = 1 + k_2\left.\frac{\partial\psi_1}{\partial p_3}\right|_{p_2=0} < 0 \tag{34}$$

Observation of Equation 31 through Equation 34 reveals that *E* is locally positive definite. Derivative of *E* is given by Equation 35.

$$\begin{aligned} \dot{E} &= \frac{\beta_1\left(p_2\right)}{\beta_3\left(p_2\right)}\dot{p}_2 + p_3\dot{p}_3 + \hbar\dot{\hbar} \\ \dot{E} &= -\frac{\alpha^2}{\delta_1^2\delta_2}\hbar^2 - \frac{\beta_2\left(p_2, p_3\right)}{\beta_3\left(p_2\right)}p_3 + \alpha\hbar p_3\frac{cos\left(p_2\right)}{\beta_3\left(p_2\right)} \end{aligned} \tag{35}$$

Noting that $\beta_3\left(p_2\right) \le -\delta_1$ for some $\delta_1 > 0$ Let us assume that,

$$\frac{\partial \psi_1}{\partial p_3}(0) < 0 \tag{36}$$

With the assumption in Equation 36, we have $\beta_2(0, p_3) \le -p_3\delta_{12}$ for some $\delta_{12} > 0$; and $\frac{\beta_2(p_2, p_3)}{\beta_3(p_2)} > p_3\delta_2$ for some $\delta_2 > 0$, hence Equation 35 results in Equation 37.

$$\dot{E} \le -\frac{\alpha^2}{\delta_1^2\delta_2}\hbar^2 - \delta_2 p_3^2 + \alpha\hbar p_3 \frac{\cos(p_2)}{\beta_3(p_2)} \tag{37}$$

Using Young's inequality, we observe that,

$$\alpha\hbar p_3 \frac{\cos(p_2)}{\beta_3(p_2)} \le p_3 \frac{\alpha\hbar}{-\delta_1} \le \frac{\delta_2}{2} p_3^2 + \frac{1}{2\delta_2}\left(\frac{\alpha\hbar}{-\delta_1}\right)^2 \tag{38}$$

Using Equation 38, we can recast Equation 37 as,

$$\dot{E} \le -\frac{\delta_2}{2} p_3^2 - \frac{\alpha^2}{\delta_1^2\delta_2}\hbar^2 \le 0 \tag{39}$$

If assumptions in Equation 24, Equation 34 and Equation 36 are satisfied then asymptotic stability of system in Equation 30 is ensured by Equation 39. Asymptotic stability of p_1 can be analysed by noting that $\dot{\zeta}(\underline{p}) = \dot{\hbar} = \dot{p}_1 - \dot{\psi}_1(p_2, p_3)$ so the dynamics of state p_1 can be described by Equation 40.

$$\dot{p}_1 = \dot{\hbar} + \dot{\psi}_1(p_2, p_3) \tag{40}$$

Integral curves of Equation 40 are given by Equation 41.

$$p_1 = \hbar + \psi_1(p_2, p_3) - \hbar(0) - \psi_1(0) + p_1(0) \tag{41}$$

Trajectories Equation 42 are asymptotically stable because of stable dynamics of Equation 30. Using Equation 29, we have immense degree of freedom to select ψ_1 as long as assumptions in Equation 24, Equation 34 and Equation 36 are satisfied. One particular choice is given by Equation 42.

$$\begin{aligned} &\underline{\rho} = [p_2 \quad p_3]^T, \quad \psi_1(p_2, p_3) = \underline{\rho}^T G(\underline{\rho})\underline{\rho} \\ &G(\underline{\rho}) = \begin{bmatrix} c_{11}(p_2, p_3) & c_{12}(p_2, p_3) \\ c_{21}(p_2, p_3) & c_{22}(p_2, p_3) \end{bmatrix} \end{aligned} \tag{42}$$

Expanding expression for ψ_1 in Equation 42, we get Equation 43.

$$\psi_1(p_2, p_3) = p_2^2 c_{11}(p_2, p_3) + p_2 p_3 c_{12}(p_2, p_3) + p_2 p_3 c_{21}(p_2, p_3) + p_3^2 c_{22}(p_2, p_3) \tag{43}$$

We make a suitable selection for G matrix entries given by Equation 44.

$$G(\underline{\rho}) = \begin{bmatrix} \gamma_1 p_2^{-1} & \gamma_3 \\ \gamma_3 & \gamma_2 p_3^{-1} \end{bmatrix} \tag{44}$$

Using Equation 43 and Equation 44, we get expression Equation 45 for ψ_1.

$$\psi_1(p_2, p_3) = \gamma_1 p_2 + \gamma_2 p_3 + 2\gamma_3 p_2 p_3 \tag{45}$$

The c variables act as free variables in Equation 45. They are selected such that desirable closed loop system dynamic response is achieved and assumptions in Equation 24, Equation 34 and Equation 36 are satisfied. These conditions are satisfied by relations in Equation 46, Equation 47 and Equation 48.

$$c_{12}(p_2, p_3) = c_{12}(p_2) \tag{46}$$

$$\gamma_2 < -\frac{1}{k_2} = -0.052 \tag{47}$$

$$(\gamma_1 + 2\gamma_3 p_3)\big|_{p=0} < 0 \tag{48}$$

We have selected values of γ_i and α given by expression in Equation 49. These values fulfill the criteria given by Equation 47 and Equation 48.

$$\begin{aligned} \gamma_1 &= -2.5, \quad \gamma_2 = -1.5 \\ \gamma_3 &= -0.4, \quad \alpha = 0.85 \end{aligned} \tag{49}$$

Using Equation 29 and Equation 45, we get continuous time feedback control algorithm as,

$$\begin{aligned} &\vartheta = \vartheta_n / \vartheta_d \\ &\vartheta_n = -\alpha(p_1 - \gamma_1 p_2 - \gamma_2 p_3 - 2\gamma_3 p_2 p_3) + (\gamma_1 + 2\gamma_3 p_3) p_3 + (\gamma_2 + 2\gamma_3 p_2) k_1 sinp_2 \\ &\vartheta_n = 1 + (\gamma_2 + 2\gamma_3 p_2) k_2 cosp_2 \end{aligned} \tag{50}$$

Partial state feedback law in Equation 6 takes the form of Equation 51 using state definitions of Equation 8.

$$e_a = \frac{1}{a_6}\left[(a_1 + a_2 \sin^2 p_2)u - a_3 p_3^2 sinp_2 + a_4 sin(2p_2) + a_5 p_1\right] \tag{51}$$

Simulation

The continuous time control algorithm in Equation 50 is simulated in the Matlab/Simulink as shown in Figure 3. The state space trajectories of system are presented in Figure 4. It is clear that off the manifold dynamics decay out with time and system converges to the invariant submanifold shown in this figure. The pendulum angle and velocity are plotted in the Figure 5 and Figure 6 respectively, and both converge to zero. The cart position and velocity are plotted in Figure 7 and Figure 8 respectively. It is evident that these dynamics are stable. The off-the-manifold dynamics are plotted in Figure 9. These dynamics decay with time towards zero, hence proving that this submanifold is attractive and invariant. The feedback linearized input and PMDC motor input voltages are plotted in Figure 10 and Figure 11 respectively. These values are realizable and within the practical limits.

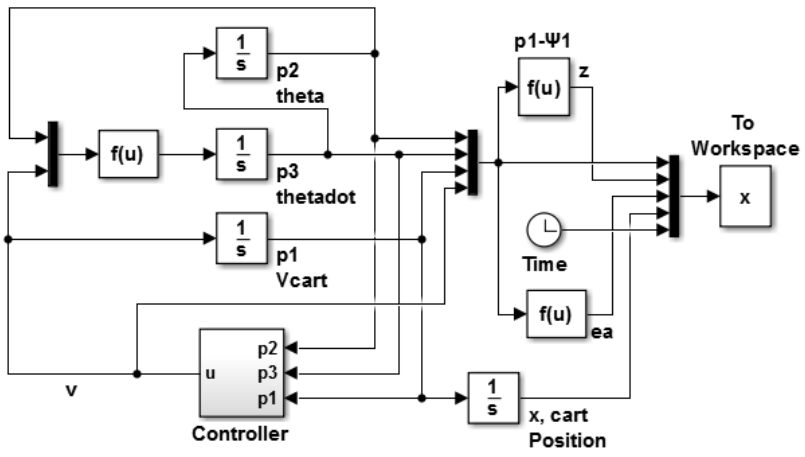

Figure 3: Continuous Control algorithm simulation

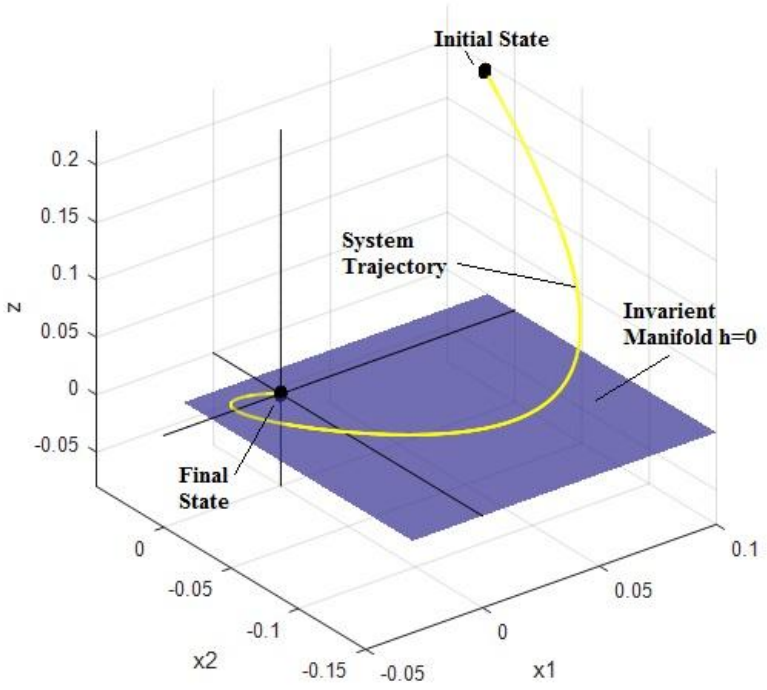

Figure 2: System trajectories and immersion submanifold

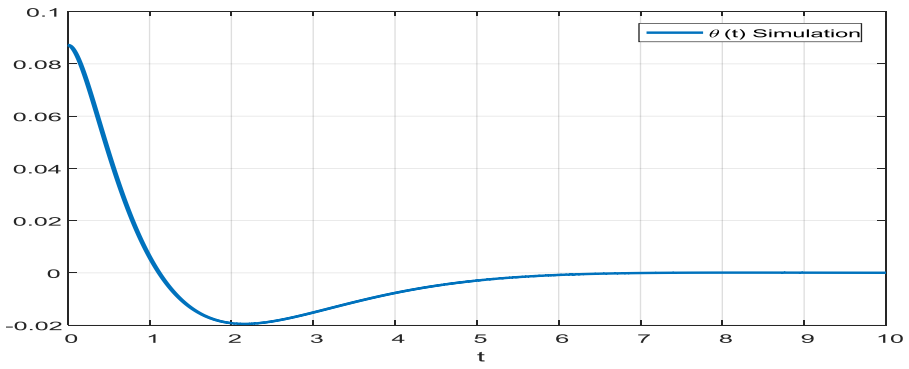

Figure 5: Responses for pendulum angle θ.

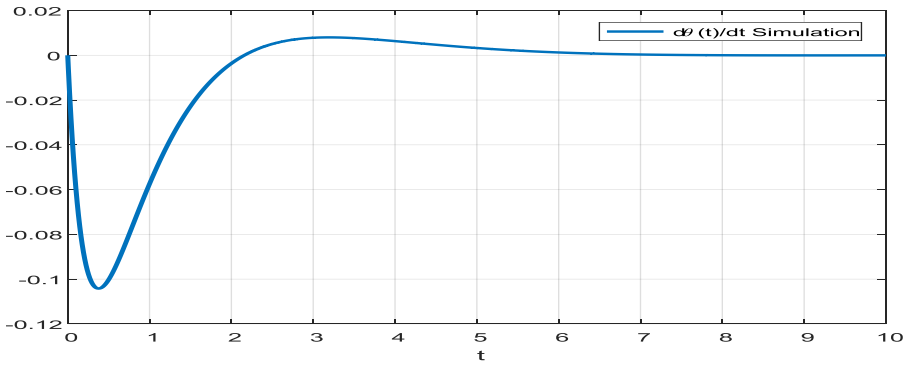

Figure 6: Responses for pendulum angular rates.

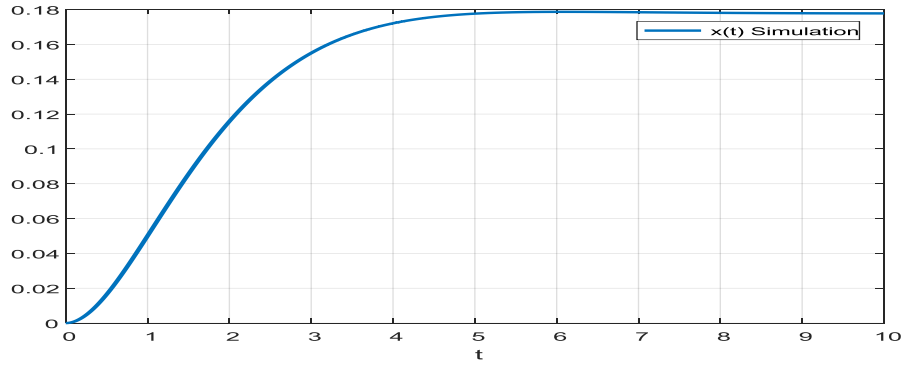

Figure 7: Responses for cart position x.

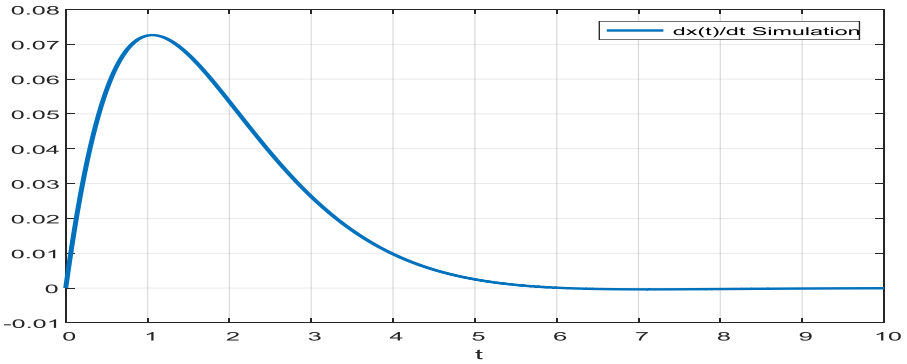

Figure 8: Responses for the cart velocity

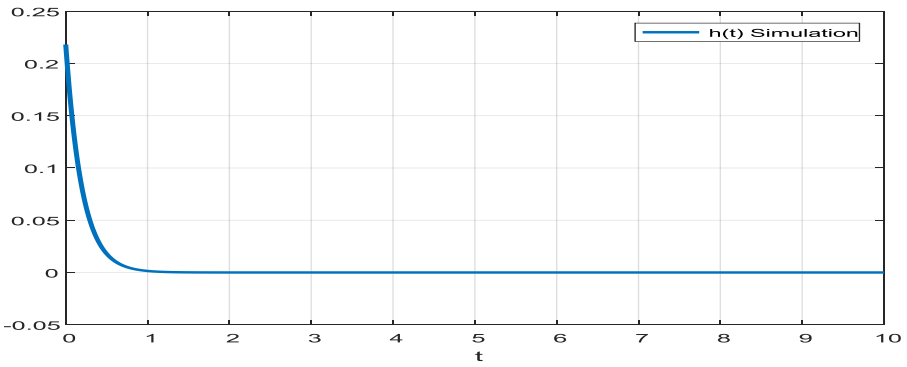

Figure 9: Responses for off-the-manifold dynamics

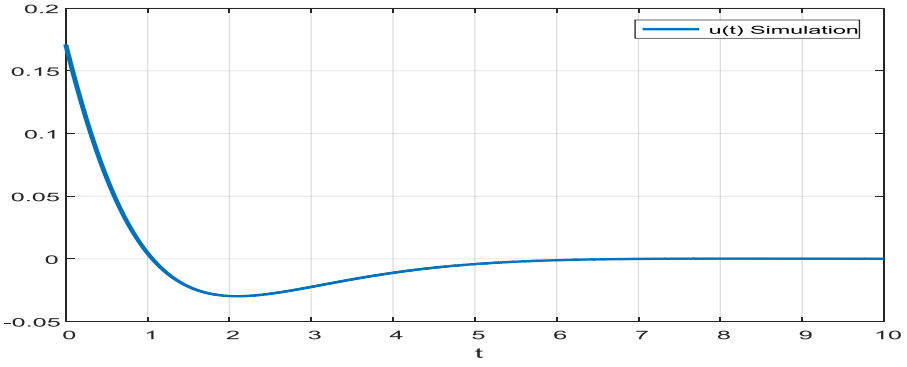

Figure 10: Feedback linearized input u

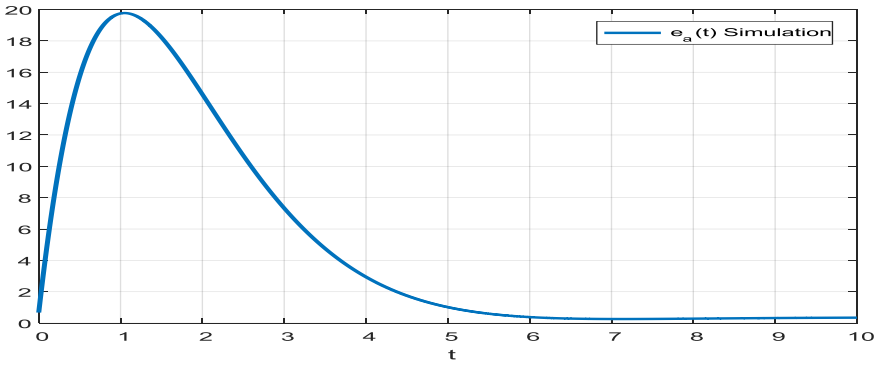

Figure 11: PMDC motor input voltage e_a

Conclusions

The robust adaptive nonlinear control approach for the compensator design of an inverted pendulum has been presented. This approach is successful in attaining the balance of the pendulum, cart position, and velocity with initial conditions of nearly horizontal pendulum angle. The proposed approach provides an immense degree of freedom in selecting the desired closed loop dynamics owing to the availability of free tunable variables in stabilizing control algorithm.

References

[1]. Oróstica.R, Duarte-Mermoud.M.A, and Jáuregui.C, 2016. Stabilization of inverted pendulum using LQR, PID and fractional order PID controllers: A simulated study. *IEEE International Conference on Automatica*, 1-7.

[2]. Pingale.S.B, Jadhav.S.P, and Khalane.V.P, 2015. Design of fuzzy model reference adaptive controller for inverted pendulum. *International Conference on Information Processing*, 790-794.

[3]. Jurdjevic.V, 1996. Geometric Control Theory. Cambridge University Press.

[4]. Astolfi.A, and Ortega.R, 2003. Immersion and invariance: a new tool for stabilization and adaptive control of nonlinear systems. *IEEE Transactions on Automatic Control*, 48(4), 590–606.

[5]. Grossimon.P.G, Barbieri.E, and Drakuno.S, 1996. Sliding mode control of an inverted pendulum. *IEEE Proceedings of the Twenty-Eighth Southeastern Symposium on System Theory*, 248-252.

[6]. Luksic.M, Martin.C, and Shadwick.W.F, 1987. Differential Geometry: The Interface between Pure and Applied Mathematics. American Mathematical Society.

[7]. Prasad.L.B, Tyagi.B, and Gupta.H.O, 2014. Optimal Control of Nonlinear Inverted Pendulum System Using PID Controller and LQR: Performance Analysis Without and With Disturbance Input. *International Journal of Automation and Computing*, 11(6), 661-670.

[8]. Hudy.W, and Jaracz.K, 2011. Selection of control parameters in a control system with a DC electric series motor using evolutionary algorithm. *Archives of Electrical Engineering*, 60(3), 231-237.

[9]. Brogan.W.L, 1985. Modern Control Theory. Prentice Hall.

[10]. Haider.A.S, Nasir.M, Safir.B, and Farooq.F, 2016. A novel ball on beam stabilizing platform with inertial sensors. *International Journal of Advanced Computer Science and Applications*, 6(8), 54-61.